SALT SPRAY TEST ON AISI 316L STAINLESS STEEL

Mariano N. Inés*, Graciela A. Mansilla
Línea de Metalurgia Física, Departamento Metalúrgica/DEYTEMA. Facultad Regional San Nicolás, Universidad Tecnológica Nacional.
Colón 332, San Nicolás de los Arroyos (2900), Pcia. Buenos Aires. Argentina

ABSTRACT

Injures produced by rigorous working conditions can affect materials, especially when they are exposed to high temperatures, corrosive atmospheres and mechanical stresses. Austenitic stainless steels have variable chromium contents but greater than 16%, which allows the surface formation of a passivating thin layer of chromium oxide (Cr_2O_3) that protects the steel against corrosion during prolonged exposure to aggressive environments.

From a metallurgical point of view, these steels meet the requirements to operate under prolonged exposures to high temperature and aggressive environments (depending on the steel grade), however attention must be paid to the precipitation of different carbides, such as $M_{23}C_6$ and M_6C, and especially sigma (σ) phase formation, since its precipitation produced chromium depleting zones which are very harmful in many applications, because it makes the material brittle and allows high corrosion penetration. Another consequence is sensitize hydrogen capture originated during corrosion.

The aim of this work is to evaluate the corrosive behavior of an austenitic stainless steel (AISI 316L) that was first exposed to several heat treatments conditions and then was subjected to a spray saline solution of 5% NaCl, inside the chamber the temperature was set in 35ºC while the saturated air temperature was 47ºC. Characterization techniques such as optical and scanning electron microscopy were applied.

Results allowed to establish the incidence on the corrosion rate of formed chromium carbides, that sensitize steel to the attack of chloride ions responsible of pitting corrosion by breaking of the passive layer thus helping a rapid corrosion rate.

Key words: **stainless steel, carbides, corrosion, salt spray chamber, piting corrosion.**

INTRODUCTION

Austenitic sainless steels are the most common and familiar types of stainless steel, because they can be made soft enough or incredibly strong by addition of alloying elements or cold working precedures. They have numerous applications, from everyday use (kitchen and food processing equipment) to the most demanding ones (including architectural applications such as roofing and cladding, heat exchangers, chemical tanks and offshore platforms). They have many advantages from a metallurgical, mechanical and corrosive point of view. Their austenitic (fcc, face-centered cubic) structure is very tough and ductile. Nevertheless, they do not lose their strength at elevated temperatures as rapidly as ferritic ones (bcc, body-centered cubic). Alloying elements accompanied by adequate heat treatments can give rise to the formation of different stoichiometries carbides, which can achieve an enhancement of the mechanical strength of these steels. However, its presence must be controlled. It is well known that continuous exposures at high temperatures result in the activation diffusion phenomena (mainly carbon and chromium) from austenitic grains to grain boundaries, producing precipitates coarsening and the creation of a microstructural state with low corrosion resistance due to a sensitization process, [1]. It is accepted that sensitivity to intergranular corrosion in austenitic stainless steels is caused by the precipitation of $Cr_{23}C_6$ at grain boundaries [2]. The formation of these carbides requires the diffusion of chromium towards grain boundaries, thus leading to the creation of a Cr-depleted zone in the vicinity of the grain boundary [3].

Stainless steels are generally very corrosion resistant and will perform satisfactorily in most environments. However, this behaviour will depend on its constituent elements when exposed to a corrosive environment, for

example, under exposure to aggressive atmospheres conditions (for example in seawater or marine atmospheres) stainless steel corrodes more than it is thought. The author in [4] stated that passivity is the ability of a metal to resist against corrosion despite the thermodynamic tendency of a metal to react with a corrosive environment. Literature suggest that exposing stainless steels to chloride enriched environment results in chloride penetrations [5] and the breakdown of the passive layer occurs at localized heterogeneities sites making the steel vulnerable to pitting corrosion and stress corrrosion cracking [2].

Although corrosion phenomena in stainless steels is not yet fully studied due to broad variety of this steel, nowadays publications mainly report corrosion degradation of mechanical properties. In this sense, several authors [3, 6, 7] stated that corrosion reduces the yield strength, ultimate strength and ductility because of hydrogen accumulation whitin steel, named as hydrogen embrittlement.

EXPERIMENTAL PROCEDURE

Chemical composition of AISI 316L staninless steel is listed in Table I.

Table I. Chemical composition of 316L stainless steel

Comp.	Fe	C	Si	Cr	Mn	Ni	Mo
Mass%	Bal.	0.032	0.65	17.2	1.50	10.7	2.57

Firstly, Table II shows different heat treatments conditios applied to the as-received samples (AR01-AR02-AR03) in order to achieve different carbides precipitation.

Table II. Heat treatments parameters

Sample	Temp. [ºC]	Time [min]	Cooling media
W1-W2-W3	900	120	Water
A1-A2-A3	900	120	Air

After that, samples were subjected to a spray saline chamber test, in a DIGIMESS Salt Fog Chamber machine Model QSS-108, according to ASTM B117 and ISO 9227 standards [8] and post-test mechanical and chemical cleaned under ASTM G1 [9]. The arrangement of samples in the salt spray chamber is shown in Figure 1.

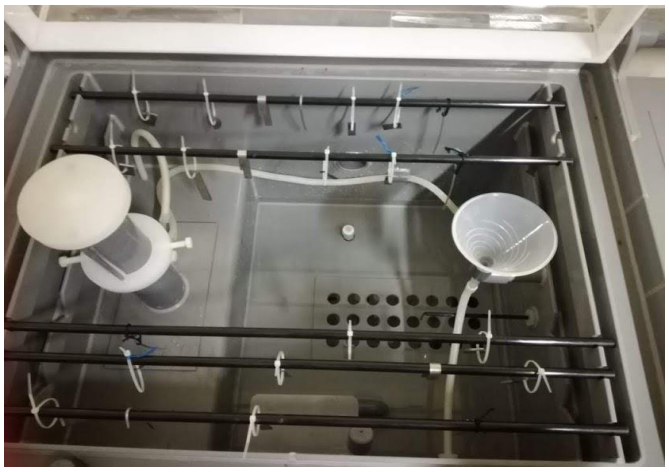

Figure 1. Samples arrangement into salt spray chamber.

Different exposure times to 5% NaCl saline spray were considered, that is, 8h, 50h and 96h respectively, Table III.

Table III. Exposure time of the saline spray for each sample

Sample	Time, [h]
AR01-W1-A1	8
AR02-W2-A2	50
AR03-W3-A3	96

At defined times, samples were taken out of the chamber in order to evaluate mass loss following the procedure explained by the authors in [10]. Finally, to assess deterioration of the material exposed to corrosion test, the corrosion rate was calculated (1).

$$\text{Corrosion rate } [\text{g/m}^2\text{h}] = \frac{\text{K} \,.\, \Delta\text{W}}{\text{A} \,.\, \text{T} \,.\, \text{D}} \qquad (1)$$

where K represents a material constant, ΔW refers to the mass lost (in grams), A is the sample tested area, T is the exposure time and D is the material density.

Samples characterization after corrosion test were carried out with magnifying glass (Olympus SZ61), optical microscope (Olympus GX51) and scanning electron microscope (Fei Modelo INSPECT S50) with energy dispersive analysis, EDS.

RESULTS AND DISCUSSION

Cooling rate-dependent microstructures as well as the amount of carbides produced by heat

treatments and surface oxides developed as a result of salt spray corrosion tests, were examined and determined. Prior corrosion tests, microstructural characterization on heat treated samples by optical microscopy and SEM/EDX was performed.

Regardless of the cooling medium of heat treated stainless steel samples, Figure 2 shows a typical microstructure of austenitic grains with carbides, mainly at grain boundaries and some inside grains. EDX analysis has been used to confirm the presence of different elements such as Fe, Cr, Ni, C, Mo, and Si forming carbides in the structure.

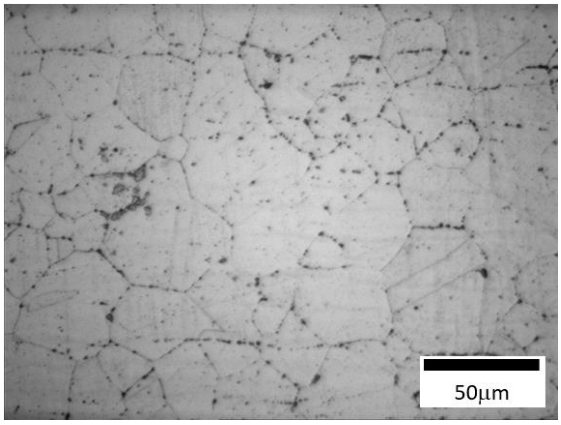

Figure 2. Optical micrograph illustrating the initial microstructure of heat treated sampes

Concerning with cooling severity and its influence on chromium carbides development, it was possible to calculate its density using image analyzer software. As a result, an increase of 1,5% in carbides amount was promoted for air cooled samples in relationship for those cooled with water. This behaviour could be attributed to the higher cooling rates that impede correct growth of chromium carbides in austenitic grain boudaries, promoting a smaller quantity of carbides developed. This is alike with what Ki-Nam Jang [11] stated about the effect of cooling rates on carbide precipitates and microstructure of 9Cr-1Mo oxide dispersion strengthened steel, also he added that carbides precipitation become smaller and more widely dispersed with increasing cooling rate.

In these sense, proposed cooling conditions provoque small influence on carbides size, as for water cooled samples they show 1 µm - 2 µm carbide size, while sizes of 1 µm - 4µm in air cooled ones were detected. Always carbides were mainly developed at austenitic grain boundaries. Type $M_{23}C_6$ steady carbide was mostly found, in accordance with thermodynamic simulation made with FactSage 7.0, [12, 13]. Another issue that indicates about these kind of precipitates, was the low chromium content near precipitates and in austenitic grain boundaries detected by EDS analysis. This fact could be attributed to a complex precipitation reaction, [14] that cause chromium depleted zones around precipitates.

After accelerated corrosion tests, a stereoscopic magnifying glass analysis was carried out for samples exposed to 50h and 96h, since they were the most long times. As result, as-received samples (i.e. without heat treatment) for both times, the presence of superficial isolated oxides were observed, as can be seen in Figure 3.

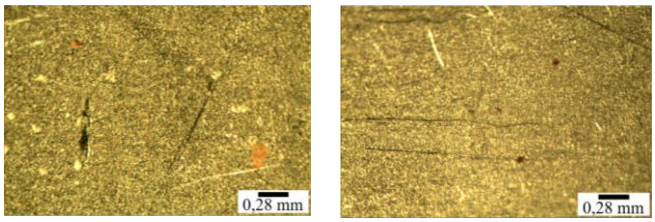

a) *b)*

Figure 3. Stereo zoom microscopy of as-received samples after corrosion test with differet time conditions: a) 50h and b) 96h.

Contrary to as-received samples, all heat treated samples have shown as exposure time increases, regardless of cooling media employed, greater amount of Fe oxides, which subsequently produces reddish rust products giving an irregular and rough surface aspect, Figure 4.

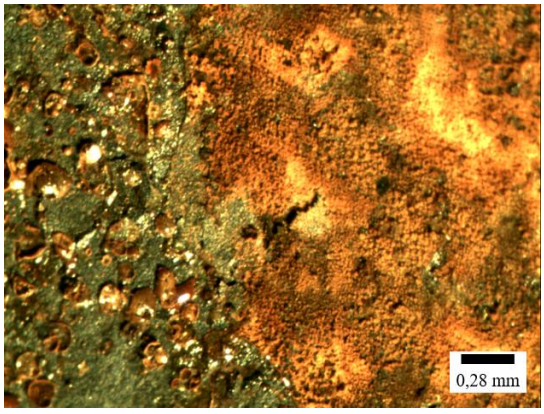

Figure 4. Oxides appearance on sample W3 (heat-treated water cooled sample and then 96h exposure to spray saline).

Figure 5 shows photos of all heat treated samples surfaces.

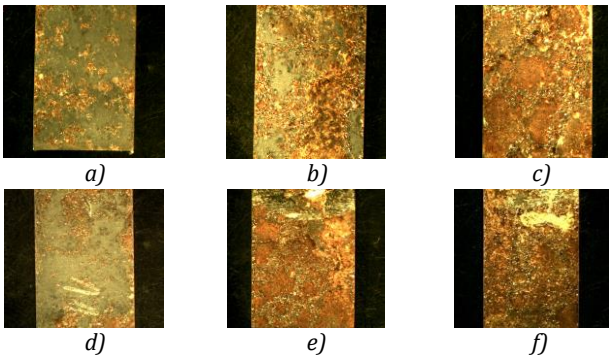

Figure 5. Surface aspect after accelerated corrosion tests on samples with prior heat tretmented. a) W1, b) W2, c) W3, d) A1, e) A2 and f) A3. Magnification [0.67x].

It must be remarked that for a minimum exposure time of 8 hours, all samples have developed greater corroded zones over the surface, but preferably on edges and around fastening holes, Figure 6.

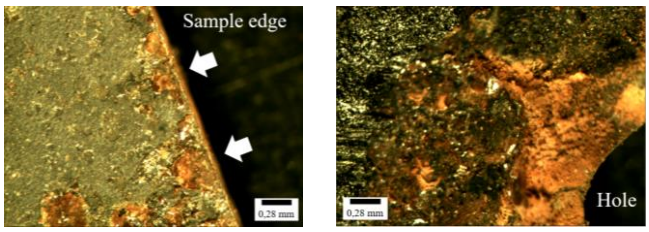

Figure 6. Corrosion process start zones on heat treated samples.

In contrast, well developed corrosion products were more evident for samples exposed 50h and 96h to the saline solution. The corroded reddish patina consists mainly of Fe oxides, as can be seen in all cases in Figure 5 (b-c-e-f).
Considering the longest exposure time (96h), it was evident that this condition has promoted an increase in the amount of surface oxides developed, as quantified in Figure 7. It was also observed that for air cooled samples corrosion products covered practically the whole sample surface, however in water cooled ones, the 88% of the surface was corroded. This could be due to the lower cooling kinetics of samples that were air cooled in contrast to those water quenched, generating a greater degree of chromium diffusion from austenitic grains to the grain boundaries, resulting in a probable greater chromium deppletion area within of austenitic grains.

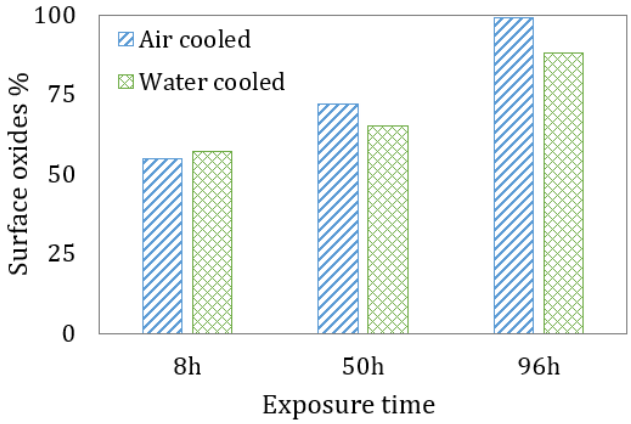

Figure 7. Quantification of surface oxides on samples as a function of spray exposure time

Optical micrographs of samples exposed to 96h saline solution are given in Figure 8. In addition, according to the methodology applied by [15] detailed crack analysis were made conducting at surface and subsurface levels, well developed cracks were found specially in samples with the longest exposure time to saline spray. As a consequence of heat treatmets, sensitized samples have shown greater corrosion damage due to chromium deppletion zones formed near grain boundary, and consequently intergranular cracks.

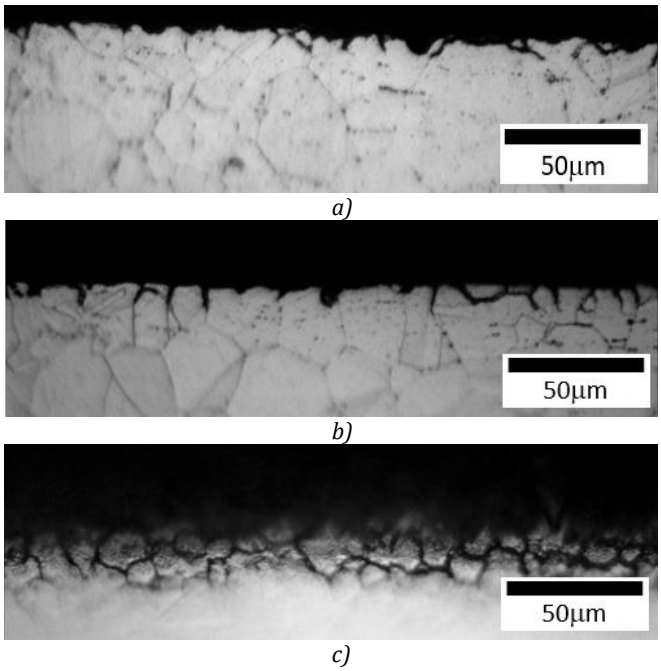

Figure 8. Crack propagation pattern in all samples tested at 96h. Noted that the integranular degradation in air cooled sample was the biggest. Sample: a) AR03, b) W3 and c) A3.

Samples profiles presented in Figure 8, clearly exhibit microstructural damage, from interganular cracks either to grains lost, when

comparing prior heat treated samples with those as received. The latter show the lowest degree of surface corrosion attack, however, very short cracks up to 4 microns associated with iron oxides were found, Figure 8a. On the other hand, for heat treated samples greater damage was observed. That is, in water cooled sample, Figure 8b, intergranular surface cracks up to 5 microns in length were observed, with corrosion pits in adjacent areas.

In air cooled samples and then corroded, Figure 8c, the highest degree of corrosion penetration was recognized, with cracks that reached up to 15 microns in length. Besides, it was determined intergranular chromium carbides linked directly to those cracks. In this way, and in accordance with [15], it could be stated that corrosion products associated with cracks would generate stresses on surface samples decreasing corrosion resistance. Neverless as it was evidenced, air-cooled samples showed the highest microstructural attack compared to all tested samples.

In concernig with corrosion rates calculated by means of equation 1, Figure 9, evidently the maximum value is reached at the first 8 hours of exposure, then decreasing and finally stabilize the accelerated attack process of the beginning.

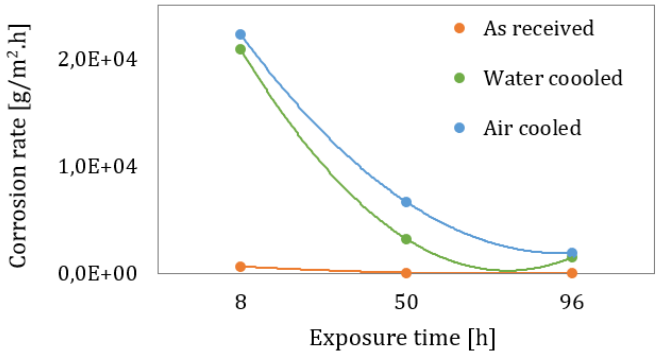

Figure 9. Corrosion rate of samples.

Such behavior could be attributed to chromium carbides precipitated inside the grains as well as those transgranular [12-16], turning austenitic grains more sensitive to chloride ions attack, thus favoring the rupture of its characteristic protective film and accelerating corrosion reaction [1,17,18]. This was verified by scanning electron microscopy (SEM) that revealed the widespread presence of corrosion pits, as well as cracks associated with intergranular corrosion and carbides as was previously mentioned.

CONCLUSION

AISI 316L heat treated samples were exposed to different times to a 5%NaCl solution in a salt spray chamber, showing different corrosion levels.

Results allowed to establish the incidence of chromium carbides on corrosion rate of these samples.

It was also clarified that time is a key factor that determines the degradation of this stainless steel. In heat-treted samples, longer exposure times have favored uniform and pitting corrosion developments. Nevertheless, corrosion rate was higher in air cooled heat treated samples as results of the greater chromium deppletion near grain boundaries and the increase in carbides amount that was promoted because of lower cooling rates.

REFERENCES

[1] Abd Rashid MW, Gakim M, Rosli ZM, Asyadi Azam M. Formation of Cr23C6 during the sensitization of AISI 304 stainless steel and its effect to pitting corrosion. Int. J. Electrochem. Science. 2012 7, 9465 – 9477.

[2] Saremi M, Mahallati E. A study on chloride-induced depassivation of mild steel in simulated concrete pore solution. Cem. Concr. Res. 2002 32, 1915-1921.

[3] John W. and Sons. Corrosion and corrosion control. Revie RW. 2008. New York,

[4] Marcus P, Maurice V. Passivity of metals and semiconductors. The Electrochemical Society, Jasper Park Lodge, Canada.1999 30–64.

[5] Román J, Vera R, Bagnara M, Carvajal A.M, Aperador W. Effect of chloride ions on the corrosion of galvanized steel embedded in concrete prepared with cements of different composition. Int. J. Electrochem. Science. 2014 9, 580-592.

[6] Marcus P. Corrosion mechanisms in theory and practice. 2011 Third ed., CRC Press Boca Raton.

[7] Eggum TJ. Hydrogen in low carbon steel: diffusion, effect on tensile properties, and an examination of hydrogen´s role in the initiation of stress corrosion cracking in a failed pipeline. 2013 (Ph.D. thesis), University of Calgary,

[8] ASTM B117 – 07. Standard Practice for Operating Salt Spray (Fog) Apparatus. 100 Barr Harbor Drive, PO Box C700, West Conshohocken, PA 19428-2959, United States. 2003.

[9] ASTM G1. Standard Practice for preparing, Cleaning, and Evaluation Corrosion Test Specimens. PO Box C700, West Conshohocken, PA 19428-2959 USA. 1999.

[10] Bertucelli MJ, Inés MN, Delpupo MN, Mansilla GA. Corrosion study in SAE 1016 electrogalvanized steel. XI Corrosion Latinamerican Congress, Latincorr. 2018 031, 23-25.

[11] Jang KN, Kim TK, Kim KT. The effect of cooling rates on carbide precipitate and microstructure of 9CR-1MO oxide dispersion strengthened (ODS) steel. Nuclear Engineering and Technology. 2019 51, 249-256.

[12] Inés M, Mansilla G. Efecto de los tratamientos térmicos en la estabilidad de carburos en aceros inoxidables AISI 316 y AISI 446. Anales CONAMET-SAM 2017, Copiapó-Chile.
[13] Inés M, Mansilla G. Estudio de la precipitación de fases en aceros inoxidables y su interacción con el hidrógeno. Anales 6° Encuentro JIM 2017, Buenos Aires, Argentina.
[14] Rozenak P, Eliezer D. Precipitation behaviour of sensitized AISI type 316 austenitic stainless steel in hydrogen. Journal of Materials Science. 1986 21, 3065 – 3070.
[15] Inés M, Asmus C, Mansilla G. Influence of total strain amplitud on hydrogen embrittlement of high strength steel. 2015 8, 1039-1046.
[16] Inés M, Mansilla G. Hydrogen trapping sites in AISI 316L and AISI 446 stainless steels. Anales of International Conference on Emerging Trends in Materials Science and Nanotechnology. 2018 Rome, Italy.
[17] Rodríguez CJ, Figueroa Y, Prin J. Efecto de la temperatura en el comportamiento del acero inoxidable austenítico 316L frente a la corrosión electroquímica. Universidad de Oriente, Venezuela. 2013 25, 3, 302-308.
[18] Afolabi A, Peleowo N. Effect of heat treatment on corrosion behaviour of austenitic stainless steel in mild acid medium. Anales de International Conference on Chemical, Ecology and Environmental Sciences. 2011.